

## **MICROBIAL PRODUCTION AND HOST DISPOSITION OF INTESTINAL CO<sub>2</sub>: INFLUENCE OF DIET AND PHYSIOLOGICAL AND PATHOPHYSIOLOGICAL EFFECTS IN THE LARGE INTESTINE**

HENRIK RASMUSSEN

GE Healthcare AS, Oslo, Norway

### **SUMMARY**

High luminal Pco<sub>2</sub> levels occur in the caecum and anterior large intestine of many species with conventional microflora, while Pco<sub>2</sub> levels equivalent to normal tissue Pco<sub>2</sub> occurs in germfree animals. Serosal Pco<sub>2</sub> is higher than normal tissue Pco<sub>2</sub> in conventional mice, which is caused by the large intestinal microflora metabolism and the inability of the caecal circulation to absorb the exogenous CO<sub>2</sub>, produced by the microflora, at sufficient speed.

Lower Pco<sub>2</sub> levels in the caecal and colonic wall of larger species (guinea pigs, rabbits and dogs), despite luminal Pco<sub>2</sub> levels comparable to or higher than in mice, are considered to be a result of a more effective vascular absorption and physical containment of the CO<sub>2</sub> produced by the large intestinal microflora.

When added to normal peripheral partial pressures of other blood gases, the high serosal Pco<sub>2</sub> levels contributes to tissue gas supersaturation in the entire depth of the affected regions of the caecal wall in mice. If blood passage through the affected parts of the caecum leaves sufficient time for equilibration of dissolved gases, gas carrier contrast agents (GCAs) used as ultrasound contrast agents present in the plasma phase of the blood will experience gas supersaturation. Under such conditions, and particularly when a significant proportion of the gases is CO<sub>2</sub>, microbubble growth will be rapid. Upon administration of GCAs in mice, vascular clearance of CO<sub>2</sub> will be compromised by vascular obstruction of microvascular beds. Other microbubbles present in the affected vascular bed will experience increased equilibration time with the supersaturated tissues, resulting in a cascading worsening and expansion of the caecal wall region affected by vascular obstruction and ischaemia in mice. The hepatic lesions observed in mice are caused by embolic distribution of large gas bubbles from the caecum via the portal vein.

The effects in rodents of exogenous CO<sub>2</sub> of microbial origin illustrate the unique features of CO<sub>2</sub> in relation to bubble growth and that local Pco<sub>2</sub> levels may deviate substantially and transiently from the normal systemic blood Pco<sub>2</sub> levels. Endogenous and exogenous sources (e.g. from intestinal microflora) of CO<sub>2</sub> may therefore have dramatic local effects on the initiation of bubble growth, even at marginally increased tissue concentrations. The contribution of CO<sub>2</sub> to gas bubble growth is particularly important during hypobaric decompress-

sion, but has also been implicated during hyperbaric decompression. As the initiation of bubble growth is essential for the clinical outcome of decompression in both humans and diving mammals, transiently increased local  $P_{CO_2}$  levels and the contribution of  $CO_2$  by the intestinal microflora should receive more attention in decompression medicine.

## INTRODUCTION

The intestinal microflora is vital to the host, both in health and disease. By its close integration in the host physiology, the distinction between host and host-derived characteristics and those of the intestinal microflora is often not only quite uncertain but also ignored. Microbial generation of nutrients, vitamins and gases, and intestinal anatomy, physiology and immune function are just some of the characteristics known in humans and conventional animals, which are dependent upon and/or interact with the intestinal microflora. By complete lack of all microflora, including that of the intestinal tract, germfree (GF) animals are fundamentally different. Germfree animals thereby serve as an important resource and baseline reference that lend them to investigations of the importance and effects of the intestinal microflora. The fact that GF animals do not eliminate  $H_2$ ,  $CH_4$  or  $H_2S$  gas (Levitt and Bond, 1970) is strong evidence for the intestinal microflora origin of these gases in conventional animals and humans. Microbial numbers and their metabolism of fermentable dietary substrate is supposedly low in the normal small intestine of conventional animals and at its highest in the large intestine, where  $CO_2$ ,  $H_2$ ,  $CH_4$  and  $H_2S$  gases are produced. Regional differences in large intestinal bacterial numbers are not indicated when measured as CFU/g intestinal content, but it is important to realise that CFU numbers reflect microbial *viability* but not *activity*. Microbial mRNA concentrations, which

reflect actively dividing and hence metabolically active bacteria, are markedly higher along the mucosal surface of the caecum in mice (Poulsen et al., 1995). The higher bacterial metabolism in the caecum is logically associated with the higher concentrations of dietary substrates entering the anterior part of the large intestine. As the intestinal gas production is directly related to microbial metabolism, the caecum and anterior parts of the large intestine is the anatomical region where the intestinal tract microflora contributes the most exogenous gas to the host. The  $CO_2$ ,  $CH_4$ ,  $H_2$  and  $H_2S$  gases are produced in the large intestine and the relative contribution in flatus is very variable (Levitt and Bond, 1970; Calloway, 1968; Levitt, 1971; Danhof et al., 1963; Saltzman and Sieker, 1968; Steggerda, 1968; Levitt and Ingelfinger, 1968). Reported gas concentrations vary markedly between individuals, not only due to different microflora compositions and activities and dietary substrate, but also as a result of the gas sampling technique. Most references have analysed the gas composition of the posterior parts of the large intestine via rectal sampling tubes (Danhof et al., 1963; Levitt, 1971; Steggerda, 1968). Due to the sampling techniques and differences in the gas characteristics (i.e. gas solubility and diffusivity); data from the posterior parts of colon and rectum are representative for these large intestinal segments only. Experimental access to, and gas sampling from, the anterior large intestine

(caecum and cranial colon) is difficult, and impossible without removing the intestinal content in a clinical setting. The composition and volumes of intestinal gases produced during normal filling in this part of the intestinal tract is hence effectively unknown in humans and rarely documented in animals.

Reports on microbial production of CO<sub>2</sub> in the large intestine of animals are scarce. Intra-colonic Pco<sub>2</sub> levels in conventional, germfree and conventionalised rats are reported to be significantly higher in conventional versus germfree and conventionalised animals (*Bornside et al., 1976*). The measurements were based on rectal introduction of a gas-sampling cannula into the colon lumen and the exact anatomical

point of sampling is hence unknown. As the anterior large intestine has the best supply of fermentable dietary substrates and highest microbial metabolism of the entire intestinal tract, the true contribution of metabolic gases from this part of the intestinal tract to the host organism is therefore largely unknown. However, recent introduction of microelectrodes has enabled measurement of Pco<sub>2</sub> for various purposes in experimental animal studies (*Antonsson et al., 1990; Rozenfeld et al., 1996; Tønnessen and Kvarstein, 1996*) and our results from measurements in the intestinal tract of various species indicate that microbial production of CO<sub>2</sub> is very high in some intestinal compartments.

## SOLUBILITY AND DIFFUSION OF GASES

The gases dissolved in tissues originate from atmospheric gases inhaled or ingested, and gases formed during metabolism. Both the host and intestinal microflora metabolism contribute to the metabolic gases, which are eliminated via the lungs or as flatulence. The gases CO<sub>2</sub>, H<sub>2</sub>, CH<sub>4</sub> and H<sub>2</sub>S are produced by the intestinal microflora, particularly in the large intestine (*Saltzman and Sieker, 1968; Levitt, 1971*). Also H<sub>2</sub>S has recently been identified as a gas produced by the host and with a multitude of effects (e.g. cardiovascular, neurological and inflammatory effects) (*Olson et al., 2006; Zanardo et al., 2006; Sivarajah et al., 2006; Lee et al., 2006*). Although nitric oxide is also a metabolic gas produced by the host, it is ignored in this context as the concentrations are significantly lower than other gases of exogenous and endogenous metabolic origin.

If gas exchange is primarily blood flow-limited, the absorption rate will

be determined primarily (but not exclusively) by effective blood solubility (and blood flow rate). If exchange is diffusion-limited, the exchange rates will vary primarily (but not exclusively) according to the gas diffusion coefficients in tissue. Absorption of intestinal gases is primarily blood flow-limited, while the absorption of gases from a subcutaneous gas pocket is an example of a primarily diffusion-limited gas exchange (*Van Liew, 1962, 1968*). Parameters describing tissue gas exchange are diffusion coefficients (e.g. Fick's diffusion coefficient [D] and Krogh's diffusion coefficient [K]) and tissue solubility (e.g. Ostwald solubility coefficient [L]). As described by (*Langø et al., 1996*), K is the product of D and L and K arises from the steady state diffusion equation (Equation 1).

Reported diffusion coefficients and tissue solubility values vary quite significantly, dependent upon the type of

**Equation 1:** Steady state gas diffusion in tissues.

$$\frac{dV}{dt} = -D \times L \times A \times \frac{dP}{dz} = -K \times A \times \frac{dP}{dz} \quad (1)$$

V: volume of gas measured at ambient temperature, A: area through which the diffusion flux is confined, P: partial pressure of the diffusing gas, and z: distance of diffusion.

tissue and conditions applied (*Langø et al., 1996*). Values of D, L and K from relevant tissues are included in Table 1. Intestinal gases will exchange across tissue-tissue and tissue-gas interfaces according to partial pressure gradients and according to gas specific transfer coefficients. Experimental exchange rates of CO<sub>2</sub>, H<sub>2</sub>, CH<sub>4</sub> and H<sub>2</sub>S between isolated intestinal segments (with intact blood supply) and surrounding tissues have been described by (*Forster, 1968; Saltzman and Sieker, 1968*) and are presented in Table 1 as equilibration half-time, transfer coefficient (k) of gas exchange, and *measured* relative rates of gas absorption. The equilibration half times, transfer coefficients and relative absorption rates of Table 1 are experimental data, measured in the small intestine. These values compare well, and best to K (and L), and are assumed to be relevant for large intestinal gas exchange. The majority of the

CO<sub>2</sub> generated in the large intestinal tract is hence absorbed by the mucosal circulation and eliminated by pulmonary exhalation. Relative diffusion velocity has also been *computed* from the physical characteristics of each gas. The computed relative diffusion velocity primarily reflects the gas-specific diffusion coefficients and is hence more relevant for diffusion-limited gas exchange (e.g. subcutaneous gas pocket). Measured and computed exchange rates of O<sub>2</sub> and CO<sub>2</sub> therefore differ. In addition to different dependence on solubility versus diffusion coefficient, this difference most likely also reflects that chemical interaction (inside RBCs) significantly increase the effective solubility of both gases and that the intestinal blood flow is related to the intraluminal Pco<sub>2</sub>, such that increasing Pco<sub>2</sub> cause increased intestinal blood flow (*Pals and Steggerda, 1966*).

## MICROBIAL CO<sub>2</sub> PRODUCTION AND INFLUENCE OF DIET

Initial measurements of the luminal Pco<sub>2</sub> in *HsdHan:NMRI* mice confirmed that the caecum is the primary site of fermentation, with remarkably higher Pco<sub>2</sub> levels in the caecum (52 kPa) versus stomach, jejunum and colon (18-23 kPa) (*Rasmussen et al., 1999a*). In all subsequent experiments, the Pco<sub>2</sub> micro-electrodes were introduced into the lumen and onto the serosa of the jejunum and caecum/colon after mid-line laparotomy. The caecum was used

in rats, guinea pigs and mice while the cranial colon was used in dogs. The tip of the intraluminal Pco<sub>2</sub> sensor was placed in the centre of the intestinal contents through anti-mesenteric incisions, generally avoiding contact with the mucosa. Two different diets were used in experiments with mice. The standard diet, used if not otherwise noted, was the SDS diet. The experimental diet was the *Diet 4012.01*. The fat, protein and energy content of the

**Table 1:** Calculated and measured tissue gas diffusion and solubility values

Gas	D 10 <sup>-5</sup> cm <sup>2</sup> / s	L ml gas/m l tissue	K 10 <sup>-5</sup> ml gas x cm <sup>2</sup> /ml tissue x s at 1 ATA	Equilibration half-time min	Transfer coefficient, k 10 <sup>-3</sup> ml/min x mmHg	Measured relative rates of absorption †	Computed relative diffusion velocity ‡
CO <sub>2</sub>	1.4	0.58	0.90	5	3.7	160	35
H <sub>2</sub> S	ND	ND	ND	12	1.6	69	130
O <sub>2</sub>	1.5	0.02 4	0.042	50	0.38	13-14	1.8
H <sub>2</sub>	ND	0.01 8	0.054	90	0.22	7-8	5.0
N <sub>2</sub>	1.3	0.01 3	0.019	97-280	0.07-0.2	1-2	1
CH <sub>4</sub>	ND	ND	ND	185	0.1	4-5	2.5

D measured in rat skeletal muscle, except O<sub>2</sub> (rat myocardium). K measured in rat skeletal muscle, except N<sub>2</sub> (cat urinary bladder). L measured in human blood plasma. D, L and K values at 37°C. ND: no data.

†: Equilibration halftime, transfer coefficient and relative rates of absorption are measured in isolated intestinal segments (with intact blood supply) in cats.

‡: Relative diffusion velocities computed from physical characteristics of the gases.

D, L and K values from (Langø et al., 1996), other data from (Forster, 1968) and (Saltzman and Sieker, 1968).

two diets are practically identical, but while the standard SDS diet contains 14% dietary fibres, 46% starch and 7% “sugars” (including glucose), the custom made *Diet 4012.01* contains no dietary fibre, no starch and 73% glucose as the only carbohydrate source.

*In vivo* Pco<sub>2</sub> levels in mice, rats, guinea pigs and dogs were remarkably high in the caecal and/or colonic lumen of all species with a normal microflora metabolism (Rasmussen et al., 1999a, 2002) (Table 2). The highest luminal Pco<sub>2</sub> levels were recorded in the colon/caecum of dogs and mice, intermediate levels were recorded in rats, guinea pigs, conventionalized germfree *KI:NMRI* mice and *HsdHan:NMRI* mice on *Diet 4012.01*, and Pco<sub>2</sub> levels equivalent to or slightly higher than normal tissue Pco<sub>2</sub> were recorded in mice with no or very limited microflora metabolism (germfree and gnotobiotic

*KI:NMRI* mice and *HsdHan:NMRI* mice after removal of the caecal content by saline flushing) (Table 1). Pco<sub>2</sub> levels, equivalent to normal tissue Pco<sub>2</sub>, were also recorded in the lumen and on the serosal side of the ileum in all species. The lumen Pco<sub>2</sub> levels in both ileum and caecum/colon were unaffected during the 5 min post mortem observation time by the blood flow stop after death. The results clearly demonstrate that Pco<sub>2</sub> levels in the caecum/colon lumen are determined primarily by microflora and dietary substrate composition. When the microflora is absent (GF) or reduced in numbers and/or metabolic activity (flushed *HsdHan:NMRI* mice), or the dietary substrate entering the caecum is reduced (*HsdHan:NMRI* mice on *Diet 4012.01*), significantly lower luminal Pco<sub>2</sub> values are observed.

**Table 2:** *In vivo* Pco<sub>2</sub> levels in caecum and colon at t=0, Jco<sub>2</sub> and sensitivity of different species and strains for GCA-induced lesions

Species/strain	N	GCA-lesions	Jco <sub>2</sub> (kPa/min)	Caecum/colon Pco <sub>2</sub> (kPa)	
				Lumen	Serosa
<i>HsdHan:NMRI</i> mice <sup>1</sup>	10	+	4.3 ± 0.5	54.5 ± 4.2	26.5 ± 2.9
<i>HsdHan:NMRI</i> mice <sup>2</sup>	8	-	1.7 ± 0.2	18.2 ± 0.9	9.7 ± 2.9
<i>Hsd:ICR</i> mice <sup>1</sup>	5	+ ①	3.7 ± 0.7	58.1 ± 10.8	12.9 ± 1.9
<i>BK:NMRI</i> mice <sup>1</sup>	6	+ ①	4.5 ± 1.0	75.7 ± 6.8	26.2 ± 3.9
“Irrigated <i>HsdHan:NMRI</i> ” mice <sup>1</sup>	6	NA	1.2 ± 0.2	10.0 ± 0.8	8.7 ± 0.4
Germfree <i>KI:NMRI</i> mice <sup>3</sup>	7	-	0.4 ± 0.1	8.7 ± 0.7	9.2 ± 0.4
Gnotobiotic <i>KI:NMRI</i> mice <sup>3</sup> †	4	NA	1.0 ± 0.2	11.0 ± 0.8	11.2 ± 0.7
Gnotobiotic <i>KI:NMRI</i> mice <sup>3</sup> ††	3	NA	0.7 ± 0.2	9.3 ± 0.3	9.6 ± 1.3
Gnotobiotic <i>KI:NMRI</i> mice <sup>3</sup> †††	3	NA	1.1 ± 0.4	11.9 ± 0.5	12.0 ± 0.6
Conventionalized germfree <i>KI:NMRI</i> mice <sup>3</sup>	8	-	2.0 ± 0.6	28.8 ± 2.7	14.4 ± 2.3
<i>Mol:SPRD</i> rats <sup>1</sup>	8	+ ②	5.3 ± 0.6	52.2 ± 2.5	8.5 ± 0.5
<i>Hsd:DH</i> guinea pigs <sup>4</sup>	7	-	3.0 ± 0.2	36.7 ± 2.3	8.9 ± 0.4
Mongrel dogs <sup>5,*</sup>	4	+ ③	0.2 ± 0.1	69.8 ± 8.9	3.9 ± 0.9
Mongrel dogs <sup>5,**</sup>	4	+ ③	0.3 ± 0.2	14.1 ± 2.8	6.3 ± 0.8

All measurements were performed in the caecum, except in dogs where colon was sampled. Pco<sub>2</sub> values are stable *in vivo* values immediately before the animals were killed. Jco<sub>2</sub> is dPco<sub>2</sub>(serosa)/dt for 5 min after death. All values are mean ± SEM. 1: SDS diet, 2: Diet 4012.01, 3: Lactamin R36 diet, 4: B&K Rabbit and Guinea Pig Maintenance Diet, 5: Purina Fit & Trim® diet, \*: intestinal content in colon, \*\*: no intestinal content in colon, n: number of animals. Gnotobiotic mice were mono-associated with †: *E. coli*, ††: *Cl. difficile*, †††: *L. acidophilus*. +: Affected by GCA-induced lesions, -: Not affected by GCA-induced lesions, NA: Not applicable. ①: Markedly lower incidence of GCA-induced lesions than in *HsdHan:NMRI* mice, ②: Caecum/colon lesions only, ③: Caecum/colon lesions only and only after 28 days repeated dosing. Table content extracted from (Dirven et al., 2003; Rasmussen et al., 1999a; Rasmussen et al., 2002), except Jco<sub>2</sub> data from all other mice strains that *HsdHan:NMRI*, which are previously unpublished data (H. Rasmussen).

## HOST DISPOSITION OF INTESTINAL CO<sub>2</sub>

The serosal Pco<sub>2</sub> levels in dogs and mice were significantly lower and higher, respectively, than all other species tested (Table 2). In the dog, serosal Pco<sub>2</sub> levels were equivalent to normal tissue Pco<sub>2</sub> and hence according to expected normal physiology. The serosal Pco<sub>2</sub> of dogs remained virtually constant for 5 min after the circulation had stopped. In addition to the high lumen/serosa Pco<sub>2</sub> ratio, the effective

washout of CO<sub>2</sub> in the colon of dogs was also demonstrated by simultaneous measurement of mucosal and luminal Pco<sub>2</sub> in two dogs. Luminal-mucosal-serosal Pco<sub>2</sub> values of 58-6-3 kPa and 51-7-4 kPa, respectively, demonstrate an extremely efficient removal of luminal CO<sub>2</sub> by the mucosal circulation.

Contrary to dogs, *in vivo* serosal Pco<sub>2</sub> levels markedly above normal tissue Pco<sub>2</sub> were recorded in mice and

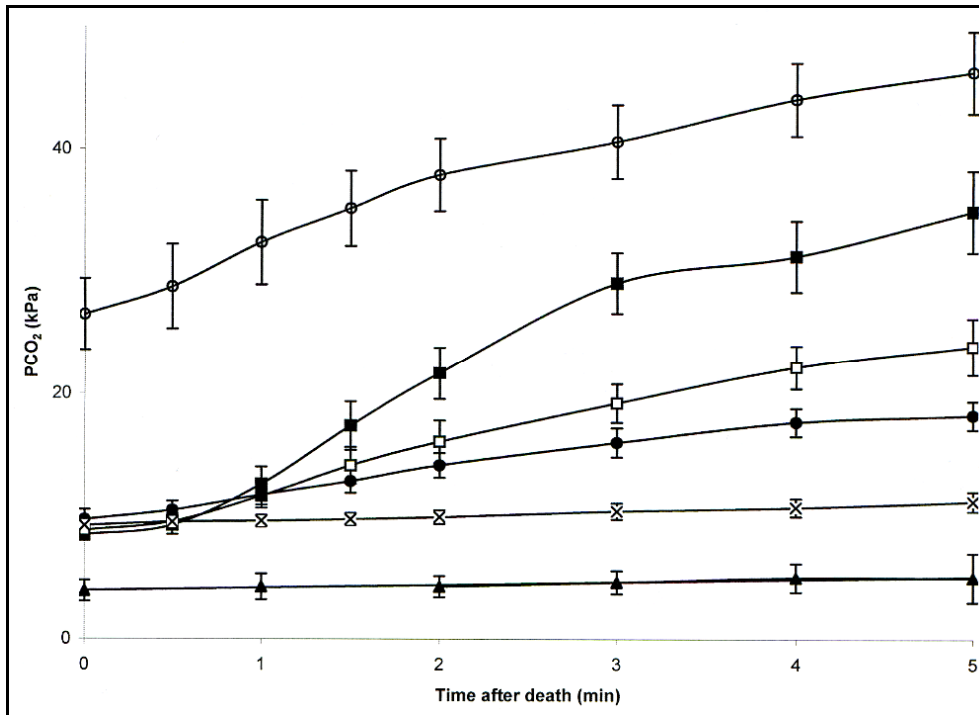


**Figure 1:** Serosal Pco<sub>2</sub> in caecum and colon.

Pco<sub>2</sub> measured in caecum in all species, except dogs (colon). Values are mean ± SEM.

○: *HsdHan:NMRI* mice on *SDS* diet (n=10), ■: *Mol:SPRD* rats (n=8), □: *Hsd:DH* guinea pig (n=7), ●: *HsdHan:NMRI* mice on *Diet 4012.01* (n=8), ×: *GF KI:NMRI* mice (n=7), ▲: Mongrel dog (n=4). Values at *t*=0 are stable *in vivo* values. Values from 0 to 5 min are post mortem values. When error bars are not shown, they are smaller than the symbols of the graph. The inclination of the serosal Pco<sub>2</sub> lines from *t*=0 to *t*=5 constitutes *Jco<sub>2</sub>* for each group. Figure previously presented in (Rasmussen et al., 2002) (without GF data) and at the Bengt E. Gustafsson Symposium, November 1, 2003, Stockholm, Sweden (unpublished).

the serosal Pco<sub>2</sub> levels increased rapidly after death. Serosal Pco<sub>2</sub> levels in rats, guinea pigs and *HsdHan:NMRI* mice on *Diet 4012.01* glucose diet were in-between these two extremes, and significantly higher than normal tissue Pco<sub>2</sub>. The lumen and serosal Pco<sub>2</sub> in rats were lower than that of mice, but the post mortem transmural increase in serosal Pco<sub>2</sub> (*Jco<sub>2</sub>*) was markedly and significantly higher. The lumen and serosal Pco<sub>2</sub> and *Jco<sub>2</sub>* were lower in guinea pigs and *HsdHan:NMRI* mice on *Diet 4012.01* glucose diet. The lumen and serosal Pco<sub>2</sub> levels in GF,

conventionalised GF and flushed *HsdHan:NMRI* mice were equivalent to that of normal tissue and the absence of a transmural Pco<sub>2</sub> gradient resulted in a low *Jco<sub>2</sub>*. These observations also confirmed that the anaesthetic (Svendesen and Carter, 1985) and surgical protocol, which was the same across all rodents, contributed little or not at all to the tissue Pco<sub>2</sub> levels recorded. The *in vivo* serosal Pco<sub>2</sub> levels and the rate of increase during the first 5 min after death (= *Jco<sub>2</sub>*) are included in Table 2 and illustrated in Figure 1.

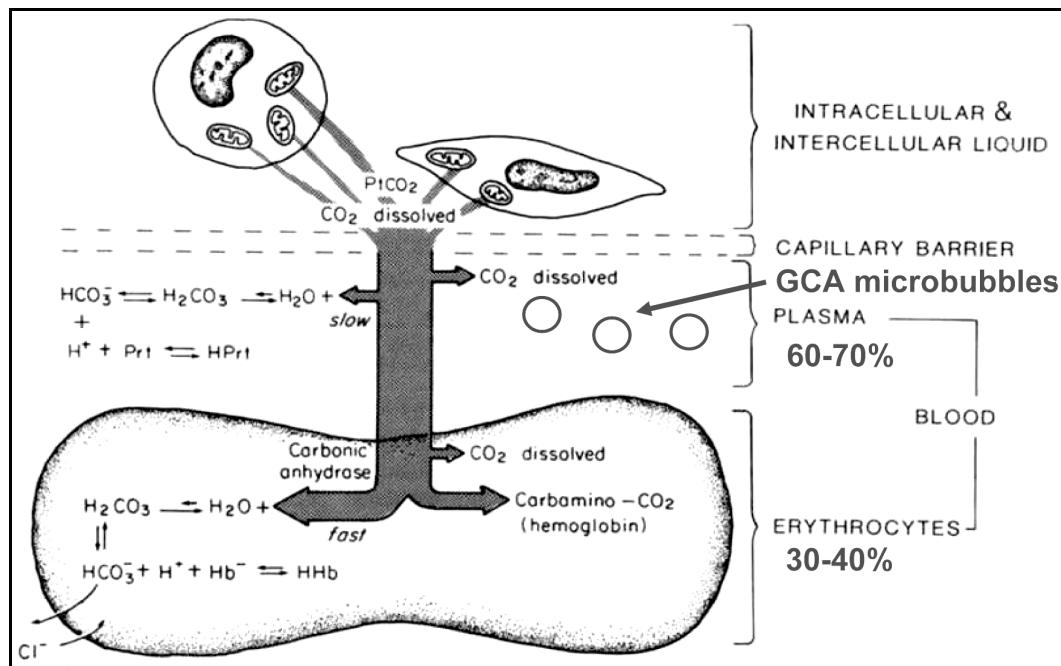


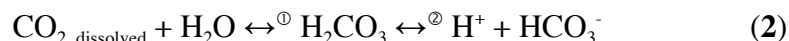
**Figure 2:** Different forms of CO<sub>2</sub> and its transportation in different blood compartments. Only dissolved CO<sub>2</sub> can cross the capillary barrier. The half-time for hydration of CO<sub>2</sub> to carbonic acid is slow without carbonic anhydrase (plasma) and rapid with carbonic anhydrase present (RBC). Dissociation of carbonic acid is spontaneous and rapid, without any enzymatic acceleration. GCA microbubbles are illustrated in the plasma space, which constitute 60-70 volume % of the whole blood. Figure modified from (Staub, 1991).

## PHYSIOLOGICAL EFFECTS OF MICROBIAL CO<sub>2</sub> PRODUCTION IN THE COLON

The physiological effects of increased serosal and intramural P<sub>co2</sub> in mice (and other rodents) during normal conditions are unknown. The high effective solubility and blood buffering of CO<sub>2</sub> is well known to maintain systemic blood P<sub>co2</sub> levels within relatively narrow limits and one may therefore question if high CO<sub>2</sub> production in the caecal lumen will be able to affect

the total gas tension in the blood as it passes through the caecal wall? The intracellular effective solubility of CO<sub>2</sub> is high due to hydration/dehydration of CO<sub>2</sub> to/from carbonic acid (H<sub>2</sub>CO<sub>3</sub>), and dissociation of carbonic acid to form bicarbonate (HCO<sub>3</sub><sup>-</sup>) and hydrogen (Equation 2). While the dissociation of carbonic acid is spontaneous and immediate (microseconds) without

**Equation 2:** Carbon dioxide reactions



①: Half-time in seconds without and milliseconds with carbonic anhydrase. ②: Spontaneous reaction with half time of microseconds.

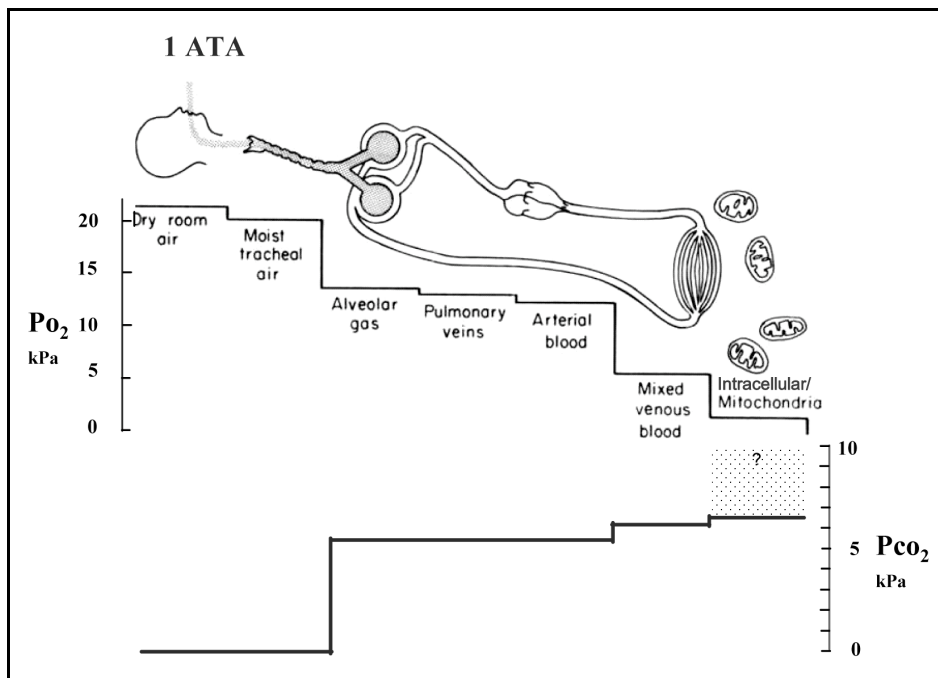


**Figure 3:** Regional  $O_2$  and  $CO_2$  tensions in different tissue compartments. The high effective solubility of  $CO_2$  results in only minor  $P_{CO_2}$  increases as oxygen is consumed. Uncertainty regarding the intracellular  $P_{CO_2}$  range (6-12 kPa) is indicated. The mitochondrial  $P_{CO_2}$  levels are unknown. Figure modified from (Staub, 1991; Hempleman, 1993).

any enzymatic acceleration, the half-time for hydration of dissolved  $CO_2$  is relatively slow without carbonic anhydrase (CA) (Staub, 1991). Carbonic anhydrase reduces the hydration half-time to milliseconds and the ability of blood to solubilize and carry large quantities of  $CO_2$  is due to the CA in RBCs. Despite the ability for rapid hydration/dissociation of  $CO_2$  in intra- and intercellular compartments, it is important to point out that  $CO_2$  can only cross cellular and organelle membranes as molecular  $CO_2$  (Klocke, 1987; Henry, 1996). Carbon dioxide can therefore only enter the blood stream across the capillary endothelium as dissolved molecular  $CO_2$  and above considerations about effective solubility are important, but yet irrelevant in this context when it occurs in the extravascular space.

In the vascular space, CA enzyme occurs in high quantities inside the RBCs but is completely absent in the plasma (Staub, 1991; Maren, 1967; Lumb, 2000). The half-time for hydration of  $CO_2$  is therefore  $>5$  sec in the plasma without CA, while the half-time is in milliseconds (Staub, 1991) and some  $13 \times 10^3 - 1 \times 10^6$  times faster inside the RBCs because of the CA enzyme (Klocke, 1987; Maren, 1967; Lumb, 2000). Although different CA iso-enzymes occur in various tissues (Sly and Hu, 1995; Maren, 1967), including the capillary endothelium and the colon, the activity and importance of these iso-enzyme is negligible when compared to the importance of CA in RBCs (Klocke, 1987). Tissue  $P_{CO_2}$  levels equal to or higher than those measured on the caecal serosal in the mouse may therefore transiently apply to the

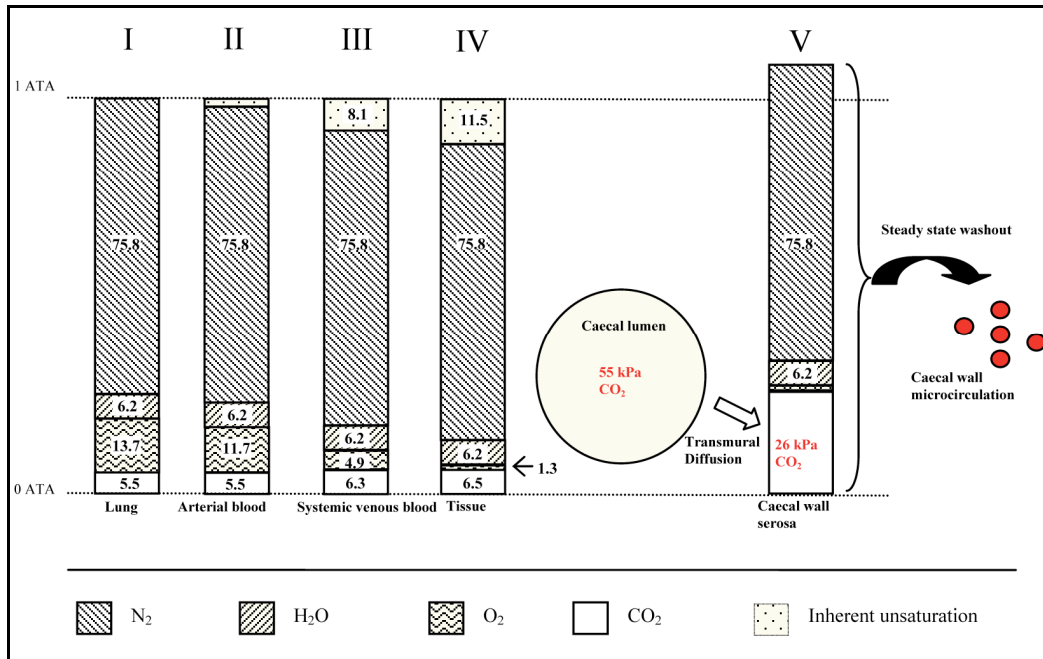


**Figure 4:** Tissue gas tensions and effects of exogenous influx of CO<sub>2</sub> into the caecal wall. The Pco<sub>2</sub> levels (kPa) of the caecal lumen and caecal wall serosa at 1 ATA are from paper II (*HsdHan:NMRI* mice). Other tissue gas tensions according to (*Hempleman, 1993; Hills, 1975*). Column numbers (I-V) indicated above columns. Figure presented with slight variations at the XIII International Symposium on Gnotobiology, June 19-24, 1999, Stockholm, Sweden (*Rasmussen et al., 1999b*), the American Ultrasound in Medicine 45<sup>th</sup> Annual Convention, March 11-14, 2001, Orlando, Florida, USA (*Rasmussen et al., 2001*) and the 2002 IAG-SOMED Joint Congress, June 14-18, 2002, Raleigh, North Carolina, USA (Unpublished).

plasma during capillary passage through discrete volumes of the caecal wall (Figure 2), while the CA enzyme in the RBCs and the haemoglobin buffering of the hydrogen ions formed during carbonic acid dissociation maintains the narrow range of Pco<sub>2</sub> in systemic whole blood.

Partial pressures of O<sub>2</sub> and CO<sub>2</sub> are regionally different (Figure 3) and are affected by metabolic consumption/production, respectively. At isobaric conditions the total tissue gas tension is hence affected by cellular metabolism, and uptake of exogenous gases originating from the intestinal tract microflora or other sources. If capillary plasma Pco<sub>2</sub> becomes transiently iden-

tical to or higher than serosal Pco<sub>2</sub> during passage through the affected caecal wall, a transient state of isobaric gas supersaturation may occur in the blood plasma.

The body is exposed to an external atmospheric gas pressure of 1 ATA or 101.3 kPa at sea level altitudes, composed in dry air of 20.2 kPa O<sub>2</sub>, 81.0 kPa N<sub>2</sub> (including 0.9 kPa argon) and a mere 36.5 Pa CO<sub>2</sub> (*Hempleman, 1993; Nunn, 1993*). After humidification of the inhaled air (Figure 4, column I) and the normally occurring ventilation/perfusion mismatch, O<sub>2</sub>, N<sub>2</sub>, H<sub>2</sub>O and CO<sub>2</sub> tensions are 11.7, 75.8, 6.2 and 5.5 kPa, respectively, and the total gas tension in the arterial blood leaving the

lungs is 2 kPa lower than that of the air inhaled (column II) (Hempleman, 1993; Hills, 1975). From this point onwards, water vapour and nitrogen remains the same throughout all tissues and further changes in total gas tension are caused by changes in O<sub>2</sub> and CO<sub>2</sub> tensions only. During tissue metabolism and O<sub>2</sub> consumption, a typical respiratory coefficient of 0.8-0.9 results in production of 0.8-0.9 moles of CO<sub>2</sub> for every mole of O<sub>2</sub> consumed. However, because the *effective* solubility of CO<sub>2</sub> (which includes both physical solubility and chemical dissociation) is considerably higher than that of O<sub>2</sub>, the resulting decrease in total gas tension is almost identical to the decrease in Po<sub>2</sub>. This difference in solubility (see Table 1 and Figure 3) result in an increasing difference between the atmospheric pressure and the total gas tension of the tissues. This difference is also known as the “inherent unsaturation” or “oxygen window” (Van Liew and Raychaudhuri, 1997; Van Liew et al., 1993; Aksnes and Rahn, 1957; Hills and LeMessurier, 1969; Lategola, 1964; Hempleman, 1993). After passage through the capillary circulation, where O<sub>2</sub> is supplied to and CO<sub>2</sub> removed from the tissues, the inherent unsaturation of the venous blood has increased to 8.0 kPa (column III). In the tissue cells (column IV), Po<sub>2</sub> and Pco<sub>2</sub> have been reported to be 1.3 and 6.5 kPa, respectively (Hempleman, 1993), resulting in a *computed* sum of partial pressures of 90 kPa and hence an inherent unsaturation of approximately 11 kPa during normal aerobic

metabolism (Hills and LeMessurier, 1969; Lategola, 1964; Hempleman, 1993; Hills, 1975). Others have reported a normal tissue Pco<sub>2</sub> of 8-12 kPa (Tønnessen, 1997) and hence a *computed* maximum inherent unsaturation of approximately 6-10 kPa. An inherent tissue unsaturation of 6-11 kPa is therefore considered to be normal during aerobic metabolism at normal atmospheric pressure.

No exogenous influx of gases is included in the above considerations about inherent unsaturation. However, if one or more exogenous gases constantly diffuse into a tissue region at sufficiently high rates, the total gas tension may increase. If the exogenous gas (e.g. CO<sub>2</sub> from the caecal lumen) constantly diffuses at high rates into a tissue region (e.g. the caecal wall) with an otherwise normal perfusion, the tissue Pco<sub>2</sub> levels may increase substantially above the normal 6-12 kPa. The increase in tissue Pco<sub>2</sub> may occur despite constant vascular absorption and disposition of CO<sub>2</sub> in the caecal wall. This exogenous CO<sub>2</sub> may be sufficient to exceed or “fill” the normal 6-11 kPa oxygen window, pushing the total tissue gas tension above 1 ATA, as illustrated in Figure 4, column V. If this CO<sub>2</sub> influx occurs in areas with a low hydrostatic blood pressure, such as the capillary vessels, post-capillary venules, veins and surrounding interstitium, gas supersaturation will occur as the total gas tension exceed the total hydrostatic pressure (atmospheric pressure + blood pressure).

### PATHOPHYSIOLOGICAL EFFECTS OF MICROBIAL CO<sub>2</sub> PRODUCTION IN THE COLON

While the normal physiological consequences of caecal gas supersaturation in mice is unknown, characteristic

pathophysiological effects will occur if mice or rats are dosed with a single dose of pre-formed gas bubbles, such

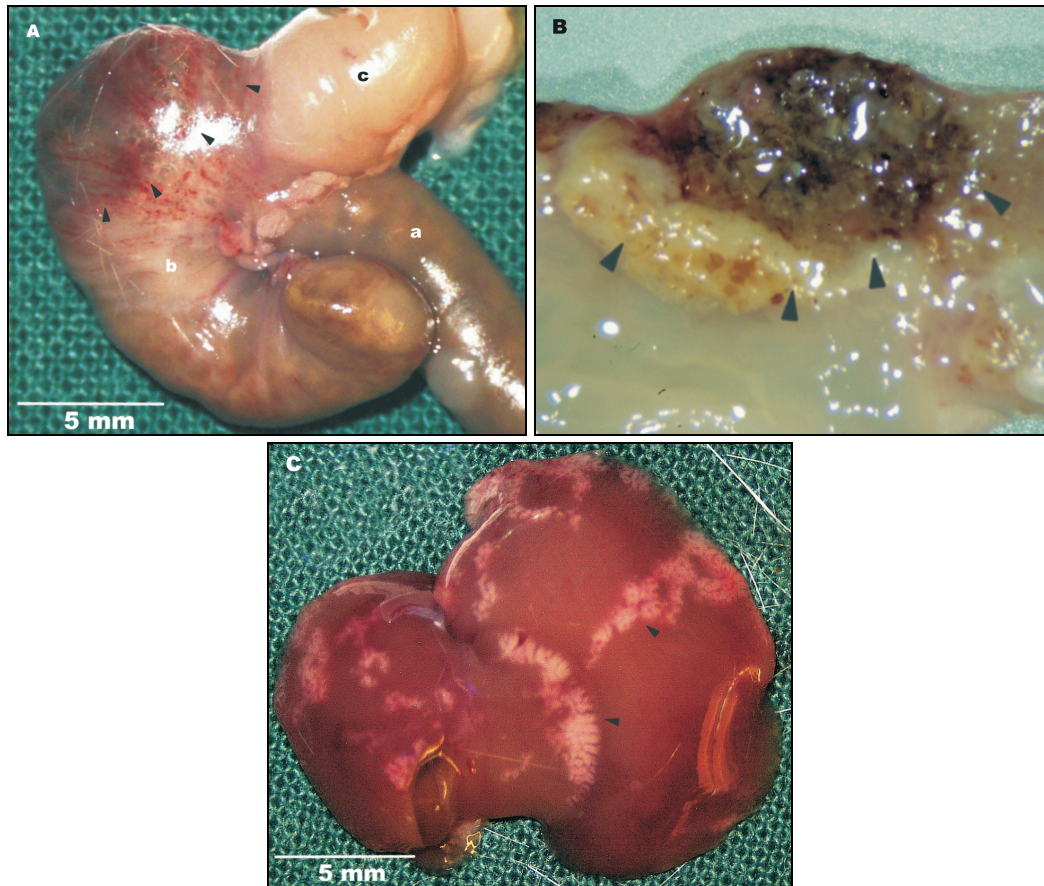


**Figure 5:** Typical macroscopic appearance of GCA-induced lesions in mice, 24 h after GCA dosing.

Ampulla coli caecum and caecocolonic area (A), caecal mucosa (B) and liver (C) of affected *HsdHan:NMRI* mice after a single i.v. injection of *Optison* (A and C) and *Sonazoid* (B) (7.5  $\mu$ l microbubbles/kg). In A, ileum (a) and cranial colon (c) is normal, while arrowheads indicate oedema and haemorrhage in the antimesenteric wall of the ampulla coli caecum (b). In B, arrowheads indicate the corresponding mucosal ulceration of caecum. In C, arrowheads indicate pale, irregular necrotic areas, often affecting the edges and surface of the liver lobes. Figure was previously published in (*Dirven et al., 2003*).

as gas-carrier contrast agents (GCAs). Gas-carrier contrast agents, which are gas microbubbles that are small enough to pass the pulmonary circulation and sufficiently pressure stable to allow passage through the left ventricle after intravenous administration, are used for contrast ultrasound imaging of the vascular system.

Characteristic necrotic lesions are observed within 24 h in the caecum,

colon and liver of mice after a single iv administration of GCAs such as *Optison*<sup>®</sup>, *Levovist*<sup>®</sup> and *Sonazoid*<sup>™</sup> (*Dirven et al., 2003*). The caecal lesions, consisting of submucosal oedema, inflammation and necrosis, appeared from 15 min and multifocal liver necrosis from 2 h after administration of GCAs (Figures 5-6). Antimesenteric and segmental predilection of submucosal oedema and lymphatic

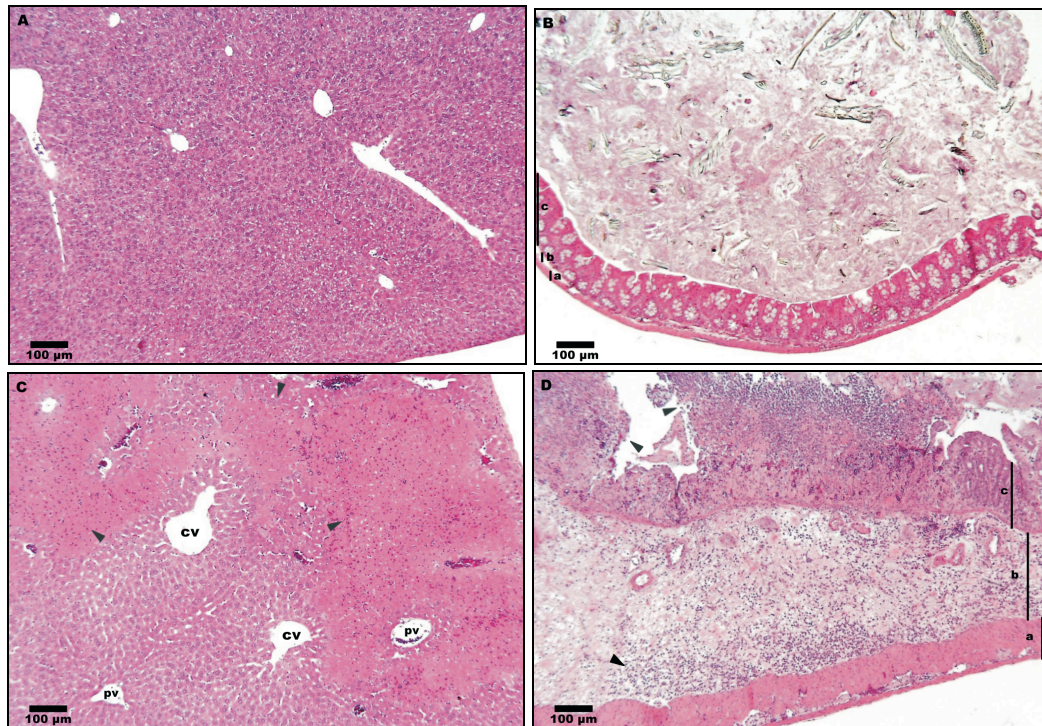


**Figure 6:** Histological appearance of liver and caecum in HsdHan:NMRI mice, 24 h after intravenous injection of Sonazoid or glucose.

Liver (A) and caecum (B) after injection of control substance (glucose). Liver (C) and caecum (D) after injection of *Sonazoid* (7.5 µl microbubbles/kg). Centrilobular coagulative necrosis indicated with arrowheads between central vein (cv) and portal vein (pv) in liver. Normal muscle layer (a) and arrowheads indicating oedema and inflammation of submucosa (b) and erosion and inflammation of mucosa (c) in caecum. This figure was previously published in *Dirven et al.*, 2003.

vessels dilatation was characteristic, particularly at the earlier time points, indicating that venous occlusion was central to the pathology of caecum and colon (*Marcuson et al.*, 1972; *Polk*, 1966; *Noonan et al.*, 1968; *Khanna*, 1959). When studied by a modified fluorescein flowmetry (FF) method 5-101 min after GCA administration, characteristic intravascular gas bubbles in and hypofluorescence of the affected caecal wall were observed in mice (*Rasmussen et al.*, 2003) (Figure 7-8). The appearance and location of the entrapped and embolic intravascular gas bubble observed by FF supported that the venous occlusion primarily oc-

curred in capillary and postcapillary venules (*Rasmussen et al.*, 1999a). The observation of intravascular gas bubbles flowing freely in intestinal veins towards the portal vein in mice, and the time course of the intestinal and liver lesion, indicate that the liver lesions are caused by embolic gas bubbles of caecal/colonic origin. This is supported by the observation that the liver lesions in mice never occurred without concurrent caecal/colonic lesions, i.e. never without a source of embolic gas bubbles. The multifocal liver abnormalities in mice, observed macroscopically as either hypofluorescence during FF or pale necrosis during 24 h pathology,

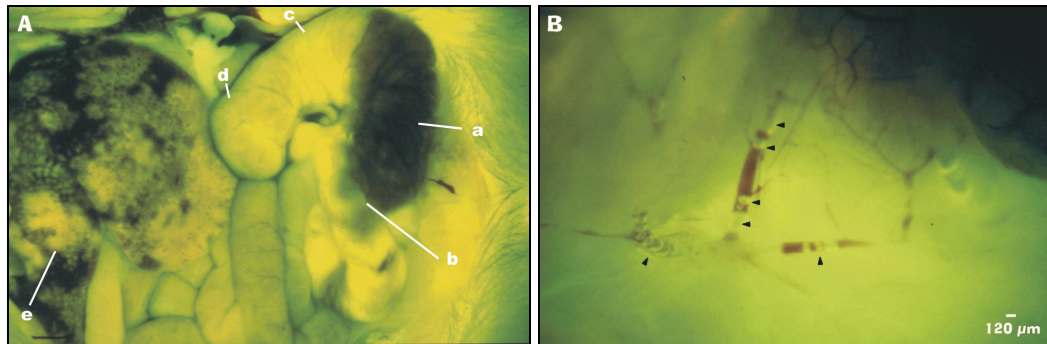


**Figure 7:** Fluorescein flowmetry in mice after intravenous administration of *Sonazoid*. Representative post mortem observation in blue light, *HsdHan:NMRI* mouse 58 min after *Sonazoid*. The animal was dosed with sodium fluoride 10 sec before it was killed. A, Abdomen, 6.5 x magnification, note non-fluorescence of antimesenteric basis caecum (a) and caecocolonic junction (b) and normal fluorescence of corpus (c) and apex caecum (d). Uniform fluorescence of all other intestines. Irregular sharply demarcated lobular fluorescence in liver (e). B, Border zone between fluorescent and non-fluorescent caecum wall, 40 x magnification. Note numerous intravascular gas bubbles in subserosal veins (arrowheads). Fluorescein flowmetry image of control animals, dosed with glucose, is illustrated in Figure 8. Figure was previously published in (*Rasmussen et al., 2003*). Video sequences, demonstrating intravascular gas bubbles and their relation to the fluorescence distribution, are available as supplementary material via [www.sciencedirect.com](http://www.sciencedirect.com).

had a characteristic peripheral distribution along the edges and surface of the liver lobes. This characteristic location of the liver lesions is consistent with that observed by ultrasound in patients with hepatic portal venous gas, in which hyperechoic signals from embolised gas bubbles are observed primarily in the periphery of the liver lobes. The peripheral and superficial location of liver gas emboli is explained by the centrifugal flow of the portal vein and is distinctly different from the deeper location and characteristic US images of gas bubbles in the centripetally flowing biliary system (*Peloponissios et al., 2003; Oktar et al., 2006; Sebastia et al., 2000; Liebman et al., 1978*). Intravital microscopy in the rat cremaster muscle after retrograde arterial administration into the femoral indicates that the intravascular behaviour and rheology of *Sonazoid* is not different from that of the white blood

cells (*Braide et al., 2006*). The vast majority of the *Sonazoid* microbubbles passed the field of view as free flowing microbubbles and the discrete and temporary plugging of the capillary circulation, which comprised 2% of the microbubbles and lasted for 3-18 seconds, was in all cases comparable to the naturally occurring leukocyte plugging (*Bagge and Brånemark, 1977*).

Histopathologically, the centrilobular hepatocyte necrosis observed in mice from 2 hours after administration of GCAs is consistent with the dual blood supply via the portal vein and the hepatic artery (*Butler and Morris, 1995*), and reperfusion injury. The centrilobular distribution is consistent with the liver necrosis of reperfusion observed in dogs 24-48 hours after transient (3 hours) episodes of severe hypovolaemia and hypotension (*Levin et al., 1996*). The centrilobular region has the lowest oxygen tension in hepatic

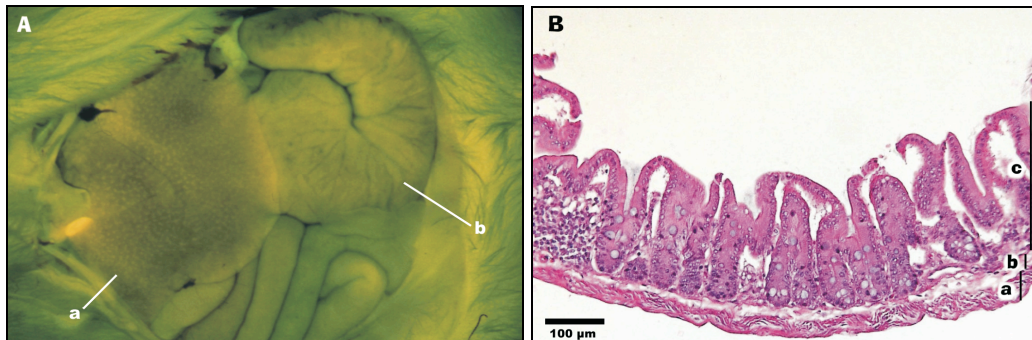


**Figure 8:** Fluorescein flowmetry in mice after intravenous administration of glucose.

A, Representative post mortem observation of abdomen in blue light, 6.5x magnification, *HsdHan:NMRI* mouse 60 minutes after administration of control substance (glucose). Sodium fluoride was dosed 10 sec before the animal was killed. Note the uniform lobular fluorescence pattern in liver (a) and uniform fluorescence of all intestines, including caecum (b). B, Representative histology of the caecum after administration of control substance (glucose), 100 x magnification, H&E. Note uniformity of the muscle layer (a), submucosa (b) and mucosa (c). Narrow space between submucosa and muscle layer is due to histological processing. Figure was previously published in (*Rasmussen et al., 2003*).

lobules and this is assumed to be the reason why this region is most severely affected by reperfusion injury following gas emboli entering the liver via the portal vein.

That presence of gas supersaturation in the caecal wall of normal mice and the causal relationship of the intestinal lesions with the disposition of the microbial CO<sub>2</sub> are also indicated by the GCA reaction in mice with reduced microflora activity. No intestinal or hepatic lesions were observed if the mice were maintained on *Diet 4012.01* for a minimum of 2 days before administration of *Sonazoid* and no lesions were observed in GF mice after administration of *Sonazoid*.

The absence of caecal lesions 24 h after single or repeated dosing of *Sonazoid* for up to 2 weeks in guinea pigs, rabbits and dogs, and the similarity of the macroscopic and microscopic caecal lesions in mice and rats divided the species into two distinct groups. Mice and rats are obviously more sensitive and although the liver is unaffected and

no abnormalities other than post mortem presence of intravascular bubbles were observed by FF in the caecum of rats, the mechanism of action leading to identical intestinal pathology at 24 h obviously shared a common mechanism in these two species. By nature and location of the scattered foci of minimal-mild submucosal inflammatory infiltration in the caecum and colon of dogs, observed after 28 days of repeated dosing of 30-1000 the clinical dose of *Sonazoid*, dogs are in principle affected by with intestinal lesions after GCA administration. However, the lesions in dogs are fundamentally different in severity, does not include liver lesions and occur only after prolonged and repeated administration of relatively high dose levels, obviously beyond clinical relevance.

What can explain the sensitivity of the mouse and rat and is this explanation relevant for the observations in dogs? The FF results clearly indicated that the GCA gas bubbles grow *in situ* in the caecum and colon wall of the

mouse and this was consistent with the observed vascular obstruction and pathology. As the volume of enlarged and entrapped gas bubbles observed in a part of the caecal wall equalled or exceeded the volume of gas contained within the administered dose of *Sonazoid*, local coalescence and/or local entrapment could not in itself explain

the pathology. The most likely source of exogenous gas responsible for bubble growth is hence CO<sub>2</sub> of bacterial origin. The nature of the initiating insults must therefore be associated with the diffusion of CO<sub>2</sub> beyond the intestinal mucosa and through the intestinal wall.

### WHAT IS EXPECTED TO OCCUR IN HUMANS?

Based on our experience with *Sonazoid*, *Optison* and *Levovist* and a number of internal and external GCA candidates (proprietary information), and the publicly available data on *Sonovue* and *Echogen*, the large intestinal and hepatic lesions are considered to be a generic trait to GCAs in the appropriately sensitive species and strain. This generic trait is observed despite quite different gas-liquid interface membranes, gas content and nature of the microbubble formation (pre-formed or de novo formation upon reconstitution). How relevant is then this generic trait of GCAs to human health?

In our measurements of large intestinal Pco<sub>2</sub>, 50-70 kPa were measured in mice, rats and dogs. In the dog (the species least sensitive to caecal/colonic lesions) 28 days repeated dosing was needed to create scattered foci of minimal-mild granulocytic foci, despite luminal Pco<sub>2</sub> levels of 70 kPa. If we assume that the hydrostatic pressure in the expandable intestine remains equal to ambient pressure, these Pco<sub>2</sub> values represent 50-70 % of the dissolved gases in the caecum and cranial colon. When the gas solubilities are also considered, gas supersaturation and intravascular growth of *Sonazoid* microbubbles in the large intestinal wall due to bacterial production of other gases than CO<sub>2</sub>, such as H<sub>2</sub>S, H<sub>2</sub> and/or CH<sub>4</sub>, is an unlikely event in human subjects.

In the event that gas supersaturation does occur in the inner-most layers of the cranial colon in some individuals, the clinical experience with *Levovist* in more than 100,000 patients (*Schlief et al.*, 1999) indicate that this is without clinically discernible consequences.

The heterogeneous delayed liver enhancement during US imaging, observed in 6 out of approximately 1500 patients dosed with different GCAs were considered a normal variant, independent of liver disease (*Okada et al.*, 2002). The anatomical location and pattern was speculated to be compatible with GCA growth or fusion in the blood vessels upstream from the portal vein. It is noted that the two GCAs (*Levovist* and *Echogen*) administered to the 6 affected patients are fundamentally very different formulations, both when compared to other GCAs and each other. Both agents are formed *de novo* immediately before administration and the degree of gas bubble membrane stabilisation is uncertain for both agents. Fusion of *de novo* forming gas microbubbles may hence be more likely than with other GCA formulations, which are all pre-formed and ready to use formulations. *Levovist* gas microbubbles are presumed to be stabilised by palmitic acid and contains relatively rapidly diffusing room air. *Echogen* contains the relatively slowly diffusing dodecafluoropentane gas and

membrane stabilisation, if any, is unknown.

Irrespective of these formulation differences, intravascular GCA growth in humans should also be considered as a possible explanation to these normal variant imaging results. When compared to the theories about pre-existing gas bubbles, intravascular GCAs represent ideal gas nuclei due to their relatively large size and the low surface tension caused by their gas-liquid interface. Lower levels of gas supersaturation will hence be needed to cause GCA growth, particularly if CO<sub>2</sub> constitutes a larger than normal proportion of the gas composition. However, the 0.4 % incidence of heterogeneous delayed liver enhancement (Okada et al., 2002) and the otherwise uneventful clinical experience after GCA administration (Schlief et al., 1999; Okada et al., 2002) make these rare observations fundamentally different from the large intestinal and hepatic lesions observed in mice and rats.

Another way of judging the human relevance is by comparing the intestinal anatomy of humans to that of the species evaluated here. Metabolically active bacteria are actively dividing bacteria and the actively dividing bacteria are often associated with the mucosal mucous layer in the anterior part of the large intestine of mice (Poulsen et al.,

1995). The mucosal area, *A*, of the anterior large intestine does therefore affect the total *active* bacterial count in this intestinal segment. The volume, *V*, of an intestinal segment determines the volume of dietary substrate available to these active bacteria on the mucosa. As the area/volume ratio is inversely related to the size of an intestinal segment, the active bacteria/dietary substrate ratio will be higher in a small caecum (e.g. mice) versus a large caecum (e.g. dogs and humans). It is also important to realize that the mucosal epithelium is one cell layer thick in all species, whilst the submucosal and muscular tunic thickness increase with increasing thickness of the intestinal wall, and the size of the species and its intestinal tract volume. Based on these anatomical differences, the observed susceptibility to large intestinal and hepatic lesions of smaller species and resistance in larger species is consistent. Decreased microflora numbers and/or metabolism as seen by dietary and antimicrobial intervention will hence reduce/eliminate the possibility of these lesions, but it is the nature of the intestinal wall which determines if and how severe the lesions will occur in a given species, even if microflora numbers and/or metabolism are increased.

#### **A WIDER PERSPECTIVE OF LOCAL P<sub>CO<sub>2</sub></sub> LEVELS AND ITS IMPORTANCE FOR *IN VIVO* BUBBLE GROWTH**

The nature and properties of inert gases in breathing mixtures used for diving are of primary concern in decompression medicine. While the inert gases are indeed the gases of highest concentration and partial pressure in both tissues and the relatively large intravascular gas bubbles associated with clinical symptoms of decompression

sickness, the importance of other and more rapidly diffusing gases during *initial* growth of micronuclei and microbubbles is largely ignored in hyperbaric decompression medicine. The solubility of CO<sub>2</sub> is exceptional among all gases present in the body, being some 20-50 times more soluble than O<sub>2</sub> and N<sub>2</sub>. While systemic P<sub>CO<sub>2</sub></sub> is nor-

mally maintained within narrow limits, even these modest partial pressures reflect relatively high concentrations of CO<sub>2</sub> and the gas concentration difference between CO<sub>2</sub> and the inert gases is therefore lower than the corresponding *partial pressure* difference. It has been demonstrated during gas supersaturation that the gases surrounding the micronucleus will leave the liquid phase and enter the gas micronucleus according to the concentration, not the partial pressure, difference across the gas-liquid interface (Hemmingsen, 1970). Carbon dioxide will hence be relatively more important in this process than indicated by the P<sub>CO<sub>2</sub></sub>. The rate of gas transport in the tissues, towards the gas bubble, and across the gas-liquid interface is dependent upon the diffusion coefficient for each of the gases in question. As demonstrated earlier (Table 2), CO<sub>2</sub> is in a class of its own with respect to solubility (L) and diffusion (K). At comparable conditions, carbon dioxide will enter gas bubbles 20-50 times faster than that of other biologically relevant gases, both during states of gas supersaturation and normal levels of inherent unsaturation (Van Liew and Burkard, 1995). Comparable dynamic or static conditions are important requirements for this comparison, as this will affect the microbubble microenvironment and hence the gas diffusion and bubble growth kinetics.

Gas bubble growth is dependent upon the initial bubble size and will occur earlier with larger bubbles (Van Liew and Raychaudhuri, 1997). The critical bubble diameter, above which the bubble grows irreversibly, depends on a number of factors, such as surface tension, hydrostatic pressure and gas concentration difference across the bubble membrane. Decreased surface tension and blood pressure, and increased gas concentration gradient will

all promote a decrease in critical diameter and hence increased chance of bubble growth at a given level of gas supersaturation. It follows from this that a sufficiently high degree of gas concentration gradient will cause bubble growth, irrespective of the bubble size. As CO<sub>2</sub> diffuse more rapidly than other gases, the entry of CO<sub>2</sub> into the gas bubble will promote early bubble growth by increased bubble diameter and decreasing the concentrations of other gases in the bubble. Enlargement beyond the critical bubble diameter and irreversible bubble growth will therefore occur at lower degrees of gas supersaturation when P<sub>CO<sub>2</sub></sub> is increased and constitutes a larger than normal proportion of the gas mixture external to the gas nucleus/bubble.

Although slower, the inert gases will also enter the gas bubble and the bubble concentration of both CO<sub>2</sub> and inert gases will eventually attain those of the surrounding tissue. Therefore, even at normal 5-6 kPa P<sub>CO<sub>2</sub></sub> in the systemic blood, the *initial* concentration of CO<sub>2</sub> in an intravascular gas bubble occurring after decompression may be considerably higher than P<sub>CO<sub>2</sub></sub> in systemic blood should indicate, and yet be equivalent to or lower than the systemic blood P<sub>CO<sub>2</sub></sub> shortly after the bubble has attained its final "stable" size.

Unfortunately, obtaining and analyzing gas bubbles immediately after formation in the tissue of origin and P<sub>CO<sub>2</sub></sub> values in the capillary plasma compartment is practically impossible. Intravascular gas bubbles are most often obtained in larger conductive blood vessels and at the earliest minutes after experimental decompression. The gas composition of these "mature" and established gas bubbles therefore reflect the systemic blood gas tensions in the larger blood vessels, rather than the initial gas concentrations in the plasma compartment of the capillary and post-

capillary circulation. The CO<sub>2</sub> concentration in the matured bubble will hence be largely equivalent to that of the systemic blood and extrapolation is needed to estimate the CO<sub>2</sub> concentration immediately after formation in the microcirculation. Extrapolation of bubble gas concentrations to the time of decompression start was included in a study of bubble formation in rabbits after severe and rapid hyperbaric decompression (Ishiyama, 1983). Gas bubbles were recovered from the vena cava at 5-15 min after decompression and analyzed so as to avoid contamination/dilution of the sampled bubbles with other gases. Gas bubble CO<sub>2</sub> concentrations and venous blood Pco<sub>2</sub> were 6-8 % and approximately 7-9 kPa, respectively, at t = 5-15 min after severe and rapid decompression, but 23% and approximately 6 kPa, respectively, at t = 0. Whilst these are extrapolated data from a rather limited study that should be judged cautiously, the importance and transient nature of CO<sub>2</sub> during early bubble is illustrated by this study.

The very early effects of mixed gases, including CO<sub>2</sub>, on bubble growth after decompression may also be mathematically modelled at microbubble diameters relevant for GCAs and the microcirculation (few μm) (Kislyakov and Kopyltsov, 1988). Hyperbaric decompression to 1/10 or 1/5 of the compressed values (corresponding roughly to 10 and 5 ATA supersaturation, respectively) and standard partial pressures of blood gases (e.g. 6.7 kPa CO<sub>2</sub>) were used. The modelling demonstrated bubble growth from 1 to 4.6 μm radius in approximately 0.12 sec after 1/10 decompression and that CO<sub>2</sub> enters the microbubble within 0.05 sec under these conditions. The rapid growth was modelled despite that the Pco<sub>2</sub> immediately after decompression were 90% of the standard 6.7 kPa

or lower, and hence not significantly higher than normal. Although based on mathematical modelling and instantaneous decompression, the applied gas mixture, bubble size and bubble density is more relevant than seen in most studies on bubble growth after decompression. The importance of CO<sub>2</sub> during initial bubble growth and the relatively higher importance of CO<sub>2</sub> at lower degrees of decompression/gas supersaturation are demonstrated.

The facilitating effects of CO<sub>2</sub> on bubble growth may also be associated with increased systemic and local levels of Pco<sub>2</sub>, as demonstrated very convincingly by Mano and D'Arrigo (1978). In a study of the DCS incidence occurring during compressed-air work in a caisson structure down to 56 m depth and 18°C on reclaimed sea bed, the rate of DCS was observed to be related to the concentration of CO<sub>2</sub> inspired during the hyperbaric decompression. The workers were experienced personnel, selected by their previous experience with caisson work and prior history of DCS. Little physical exercise was associated with the caisson work itself and the workers rested during decompression in the decompression lock, but going up a spiral stair from the caisson bottom to the decompression lock at the end of each shift was a physical strain that increased with depth and compression. Maximum compression was 3.9 ATA and signs of DCS stated to occur from 2.7 ATA. The compression lock temperature was 30°C. At compression below 3.2 ATA, the decompression lock was not ventilated and the CO<sub>2</sub> concentrations were therefore 1.8-2.3%. At compression above 3.2 ATA, the compression lock was ventilated and the CO<sub>2</sub> concentrations dropped to 0.3-0.8%. The normal atmospheric CO<sub>2</sub> concentration is 0.03%, which was also the CO<sub>2</sub> concentration in the

caisson structure. Despite the increasing compression, the modest reduction in inspired CO<sub>2</sub> concentration caused the DCS incidence to drop from 3.05% at 3-3.2 ATA to 0.96% at 3.2-3.4 ATA. The DCS incidence increased at increasing depths above 3.2 ATA, but the DCS incidence at 3.2-3.9 ATA was still below that observed at 3-3.2 ATA. The vast majority of symptoms occurred in the knees, which was thought to be associated with the hard physical exercise associated with climbing up to the decompression lock. As the workers rested in the decompression lock, local CO<sub>2</sub> production during climbing, rather than decreased hydrostatic pressure associated with muscle activity (tribonucleation), is considered to be the primary factor associated with bubble growth and the observed cases of DCS. Even at these modestly increased CO<sub>2</sub> concentrations of the breathing gas in the decompression lock, the results indicate that presumed reduced pulmonary elimination (systemic effect) and increased production (local effect in muscles around knee joint) of CO<sub>2</sub> facilitated increased tissue concentrations of CO<sub>2</sub> and caused early bubble growth during hyperbaric decompression. In addition, although the core body temperature was probably not decreased while in the caisson, the physical exercise of climbing the stairs and the markedly increased compression lock temperature may have increased local and/or systemic body temperature, causing the solubility of CO<sub>2</sub> (but not N<sub>2</sub>) to decrease. This principle of temperature-dependent gas solubility is well known in deep sea saturation diving, where hypothermia and physical exercise contributes to an increased partial pressure of metabolic gases when normal body temperature is regained in the compression chamber.

Diving mammals are able to dive to extreme depths and lengths (*Kooyman*

and *Ponganis*, 1998) and it is quite controversial if they are affected by DCS (*Jepson et al.*, 2003; *Piantadosi and Thalmann*, 2004). The ability to undertake such extreme physical exercise is primarily associated with a higher volume of blood and blood cells, haemoglobin and myoglobin, such that 80-90 % of the O<sub>2</sub> stores are located in the blood and muscles and not in the lungs (*Kooyman and Ponganis*, 1998). Redistribution of blood perfusion from the visceral organs to the central nervous system and the heart has been observed in seals during prolonged restraint dives (*Kooyman and Ponganis*, 1998). This “diving reflex” is assumed to enable the extreme diving capabilities of some seals and to occur in other mammals during unrestrained diving, but experimental verification is lacking. Uptake of gases at increased pressure occur from start of diving and until the lung collapse and repeated diving to the depth of lung collapse or lower has been shown to cause gas supersaturation in unrestrained dolphins (*Ridgway and Howard*, 1979). Based on simulation in other whale species, the degree of gas supersaturation developing in diving mammals will hence dependent upon frequency and depth of diving, surface time between diving, rates of descent and ascent and depth of lung collapse (*Houser et al.*, 2001). As bubble growth is known to be enhanced by rectified diffusion when exposed to acoustic energy of sufficient magnitude (*Crum and Hansen*, 1982), exposure of diving mammals (including humans) to high acoustic pressure may represent a risk (*Crum and Mao*, 1996; *Houser et al.*, 2001). Mass stranding of whales has been associated with the use of military sonar (*Jepson et al.*, 2003; *Fernández et al.*, 2005) and the observation of high volumes of intravascular gas bubbles in the liver,

intestines, mesenteric lymph nodes and other visceral organs has been suggested by *Jepson et al.* (2003, 2005) and *Fernández et al.* (2005) to indicate that a DCS-related aetiology may be involved. Contrary to this view, the location large gas bubble volumes of both chronic and acute nature in the liver and the diving reflex has been argued to contradict an aetiology of DCS by nitrogen gas supersaturation (*Piantadosi and Thalmann*, 2004).

The pathogenesis of these distinctive intestinal and hepatic lesions of intravascular gas bubbles remains unknown, but a theory of facilitation by metabolic gases can be discussed. If metabolic gases, and not only nitrogen, were considered in diving mammals, the distinctive intestinal and hepatic location of the intravascular gas bubbles could perhaps be associated with metabolic gases of intestinal microflora origin, in principle as outlined in the present thesis. The intestinal tract of whales is obviously very different from rodents, but fermentation of the dietary substrate and production of CO<sub>2</sub> by the intestinal microflora will be largely constant during diving and it is therefore interesting that large amounts of

fresh gastric content were observed in stranded whales with the above lesions in liver and intestinal tract (*Fernández et al.*, 2005). This metabolic gas production will accumulate locally in the intestinal tract tissue and in the systemic circulation until the animal again can exhale the gases upon surfacing. If the diving reflex applies to whales, the CO<sub>2</sub> will primarily accumulate in the splanchnic blood and tissues and relatively high Pco<sub>2</sub> levels will hence enter the portal circulation as splanchnic perfusion is normalised. If the diving mammal is exposed to high energy sonar shortly before or after normalization of the splanchnic perfusion, the increased Pco<sub>2</sub> in splanchnic and/or systemically may lower the threshold for bubble growth (*Van Liew and Raychaudhuri*, 1997; *Mano and D'Arrigo*, 1978) and intravascular bubble growth may be triggered in the portal tract and liver. If such sonar triggering of portal bubble growth in whales occurs repeatedly, a mixed chronic and acute pattern of hepatic cavitation by gas emboli, as observed by (*Jepson et al.*, 2003, 2005; *Decker*, 1990), may eventually occur and may contribute to the death and/or stranding of the animal.

## ACKNOWLEDGEMENT

Sincere thanks are due to my collaborators and co-authors on previous publications; Tore Midtvedt, Tor Inge Tønnessen, Peyman Mirtaheri, Gunnvald Kvarstein, Magnus Braide, Ulf Bagge, Ann Albrektsson, Hubert Dirven, Derek Grant, Helge Johnsen, Per Walday and Signe Videm. The skillful technical assistance by Arshad Mohammed, Brit Engebretsen, Bente Spilling, Ann Svendsen Langøy, Aud Skiphamn, Ove M. Moen, Eva Gustavsson, Eva Østerlund and Johannes Bergstedt is also greatly acknowledged and appreciated.

## LITERATURE

- Aksnes, A. and Rahn, H.: Measurement of total gas pressure in blood. *J. Appl. Physiol.* 10,173-178 (1957).
- Antonsson, J.B., Boyle, C.C., Kruithoff, K.L., Wang, H., Sacristan, E. Rothschild, H.R., and Fink, M.P.: Validation of tonometric

- measurement of gut intramural pH during endotoxemia and mesenteric occlusion in pigs. *Am. J. Physiol.* 259, G519-G523 (1990).
- Bagge, U. and Brånemark, P.-I.: White blood cell rheology. *Adv. Microcirc.* 7, 1-17 (1977).
- Bornside, G.H., Donovan, W.E., and Myers, M.B.: Intracolonic tensions of oxygen and carbon dioxide in germfree, conventional and gnotobiotic rats. *Proc. Soc. Exp. Biol. Med.* 151, 437-441 (1976).
- Braide, M., Rasmussen, H., Albrektsson, A. and Bagge, U.: Microvascular behaviour and effects of Sonazoid™ microbubbles in the cremaster muscle of rats after local administration. *J. Ultrasound Med.* 883-890 (2006).
- Butler, B.D. and Morris, W.P.: Transesophageal echocardiographic study of decompression-induced venous gas emboli. *Undersea Hyperbaric Med.* 22, 117-128 (1995).
- Calloway, D.H.: Gas in the alimentary canal. In: *Handbook of Physiology, Sec. 6: Alimentary Canal, Vol. 5: Bile; Digestion; Ruminal Physiology* (Code, C.F. and Heidel, W., Eds.). American Physiological Society, Washington D.C., 2839-2859 (1968).
- Crum, L.A. and Hansen, G.M.: Growth of air bubbles in tissues by rectified diffusion. *Physics Med. Biol.* 27, 413-418 (1982).
- Crum, L.A. and Mao, Y.: Acoustically enhanced bubble growth at low frequencies and its implications for human diver and marine mammal safety. *J. Acoust. Soc. Am.* 99, 2898-2907 (1996).
- Danhof, I.E., Douglas, F.C., and Rouse, M.O.: Mechanisms of intestinal gas formation with reference to carbondioxide. *South. Med. J.* 56, 768-776 (1963).
- Decker, K.: Biologically active products of stimulated liver macrophages (Kupffer cells). *Eur. J. Biochem.* 192, 245-261 (1990).
- Dirven, H., Rasmussen, H., Johnsen, H., Videm, S., Walday, P., and Grant, D.: Intestinal and hepatic lesions in mice, rats and other laboratory animals after intravenous administration of gas-carrier contrast agents used in ultrasound imaging. *Toxicol. Appl. Pharmacol.* 188, 165-175 (2003).
- Fernández, A., Edwards, J.F., Rodríguez, F., Espinosa de Los Monteros, A., Herráez, P., Castro, P., Jaber, J.R., Martin, V., and Arbelo, M.: "Gas and fat embolic syndrome" involving a mass stranding of beaked whales (family Ziphiidae) exposed to anthropogenic sonar signals. *Vet. Pathol.* 42, 446-457 (2005).
- Forster, R.E.: Physiological basis of gas exchange in the gut. *Ann. N. Acad. Sci.* 150, 4-12 (1968).
- Hemmingsen, E.A.: Supersaturation of gases in water. Absence of cavitation on decompression from high pressure. *Science* 167, 1493-1494 (1970).
- Hempleman, H.V.: History of decompression procedures. In: *The physiology and medicine of diving* (Bennet, P. and Elliott, D., Eds.). W.B. Saunders Company, Ltd., London, 342-375 (1993).
- Henry, R.P.: Multiple roles of carbonic anhydrase in cellular transport and metabolism. *Ann. Rev. Physiol.* 58, 523-538 (1996).
- Hills, B.A.: Biophysical aspects of decompression. In: *The physiology and medicine of diving and compressed air work* (Bennett, P.B. and Elliott, D.H., Eds.). Williams and Wilkins Co, Baltimore, 366-391 (1975).
- Hills, B.A. and LeMessurier, D.H.: Unsaturation in living tissue relative to the pressure and composition of inhaled gas and its significance to decompression theory. *Clin. Sci.* 36, 185-195 (1969).
- Houser, D.S., Howard, R., and Ridgway, S.: Can diving-induced tissue nitrogen supersaturation increase the chance of acoustically driven bubble growth in marine mammals? *J. Theor. Biol.* 213, 183-195 (2001).
- Ishiyama, A.: Analysis of gas composition of intravascular bubbles produced by decompression. *Bull. Tokyo Med. Dent. Univ.* 30, 25-35 (1983).
- Jepson, P.D., Arbelo, M., Deaville, R., Patterson, I.A.P., Castro, P., Baker, J.R., Degollada, E., Ross, H.M., Herráez, P., Pocknell, A.M., Rodríguez, F., Howie, F.E., Espi-

- nosa, A., Reid, R.J., Jaber, J.R., Martin, V., Cunningham, A.A., and Fernández, A.: Gas-bubble lesions in stranded cetaceans. *Nature* 425, 575-576 (2003).
- Jepson, P.D., Deaville, R., Patterson, I.A.P., Pocknell, A.M., Ross, H.M., Baker, J.R., Howie, F.E., Reid, R.J., Colloff, A., and Cunningham, A.A.: Acute and chronic gas bubble lesions in cetaceans stranded in the United Kingdom. *Vet. Pathol.* 42, 291-305 (2005).
- Khanna, S.D.: An experimental study of mesenteric occlusion. *J. Path. Bact.* 77, 575-590 (1959).
- Kislyakov, Yu.Ya. and Kopyltsov, A.V.: The rate of gas-bubble growth in tissue under decompression. *Mathematical modelling. Resp. Physiol.* 71, 299-306 (1988).
- Klocke, R.A.: Carbon dioxide transport. In: *Handbook of physiology, Section 3: The respiratory systems.* (Fishman, A.P., Ed.). American Physiological Society, Bethesda, MD, 173-197 (1987).
- Kooyman, G.L. and Ponganis, P.J.: The physiological basis of diving to depth: Birds and mammals. *Annu. Rev. Physiol.* 60, 19-32 (1998).
- Langø, T., Mørland, T., and Brubakk, A.O.: Diffusion coefficients and solubility coefficients for gases in biological fluids and tissues: A review. *Undersea Hyperb. Med.* 23, 247-272 (1996).
- Lategola, M.T.: Measurement of total pressure of dissolved gas in mammalian tissue *in vivo*. *J. Appl. Physiol.* 19, 322-324 (1964).
- Lee, S.W., Hu, Y.S., Hu, L.F., Lu, Q., Dawe, G.S., Moore, P.K., Wong, P.T., and Bian, J.S.: Hydrogen sulphide regulates calcium homeostasis in microglial cells. *Glia* 54, 116-124 (2006).
- Levin, S., Bienvenu, J.G., and Ostrout, M.: Have you seen this? Hypovolemic shock. *Toxicol. Pathol.* 24, 529 (1996).
- Levitt, M.D.: Volume and composition of human intestinal gas determined by means of an intestinal washout technique. *New Engl. J. Med.* 284, 1394-1398 (1971).
- Levitt, M.D. and Bond, J.H.: Volume, composition, and source of intestinal gas. *Gastroenterology* 59, 921-929 (1970).
- Levitt, M.D. and Ingelfinger, F.J.: Hydrogen and methane production in man. *Ann. NY Acad. Sci.* 150, 75-81 (1968).
- Liebman, P.R., Patten, M.T., Manny, J., Benfield, J.R., and Hechtman, H.B.: Hepatic-portal venous gas in adults: Etiology, pathophysiology and clinical significance. *Ann. Surg.* 187, 281-287 (1978).
- Lumb, A.B.: Carbon dioxide. In: *Nunn's applied respiratory physiology* (Lumb, A.B., Ed.). Butterworth-Heinemann, Oxford, 222-248 (2000).
- Mano, Y. and D'Arrigo, J.S.: Relationship between CO<sub>2</sub> levels and decompression sickness. Implications for disease prevention. *Aviat. Space Environ. Med.* 49, 349-355 (1978).
- Marcuson, R.W., Stewart, J.O., and Marston, A.: Experimental venous lesions of the colon. *Gut* 13, 1-7 (1972).
- Maren, T.H.: Carbonic anhydrase: Chemistry, physiology and inhibition. *Physiol. Rev.* 47, 595-781 (1967).
- Noonan, C.D., Rambo, O.N., and Margulis, A.R.: Effects of timed occlusions at various levels of mesenteric arteries and veins: Correlative study of arteriographic and histologic patterns of rat gut. *Radiology* 90, 99-106 (1968).
- Nunn, J.F.: The atmosphere. In: *Nunn's Applied Respiratory Physiology* (Lumb, A.B. and Nunn, J.F., Eds.). Butterworth-Heinemann, Oxford. 3-14 (1993).
- Okada, M., Albrecht, T., Blomley, M.J., Heckemann, R.A., Cosgrove, D.A., and Wolf, K.-J.: Heterogeneous delayed enhancement of the liver after ultrasound contrast agent injection - A normal variant. *Ultrasound Med. Biol.* 28, 1089-1092 (2002).
- Oktar, Ö.S., Karaosmanoglu, D., Yücel, C., Erbas, G., İlkme, A., Canpolat, I., and Özdemir, H.: Portomesenteric venous gas: Imaging findings with an emphasis on sonography. *J. Ultrasound Med.* 25, 1051-1058 (2006).
- Olson, K.R., Dombkowski, R.A., Russell, M.J., Doellman, M.M., Head, S.K., Whitfield,

- N.L., and Madden, J.A.: Hydrogen sulfide as an oxygen sensor/transducer in vertebrate hypoxic vasoconstriction and hypoxic vasodilation. *J. Exp. Biol.* 209, 4011-4023 (2006).
- Pals, D.T. and Steggerda, F.R.: Relation of intrainestinal carbon dioxide to intestinal blood flow. *Am. J. Physiol.* 210, 893-896 (1966).
- Peloponissios, N., Halkic, N., Pugnale, M., Jornod, P., Nordback, P., Meyer, A., and Gillet, M.: Hepatic portal gas in adults: Review of the literature and presentation of a consecutive series of 11 cases. *Arch. Surg.* 138, 1367-1370 (2003).
- Piantadosi, C.A. and Thalmann, E.D.: Whales, sonar and decompression sickness. *Nature* 428, 1-2 (2004).
- Polk, H.C.: Experimental mesenteric venous occlusion. III. Diagnosis and treatment of induced mesenteric venous thrombosis. *Ann. Surg.* 163, 432-444 (1966).
- Poulsen, L.K., Licht, T.R., Rang, C., Krogfelt, K.A., and Molin, S.: Physiological state of *Escherichia coli* BJ4 growing in the large intestines of streptomycin-treated mice. *J. Bacteriol.* 177, 5840-5845 (1995).
- Rasmussen, H., Kvarstein, G., Johnsen, H., Dirven, H., Midtvedt, T., Mirtaheri, P., and Tønnessen, T.I.: Gas supersaturation in the cecal wall of mice due to bacterial CO<sub>2</sub> production. *J. Appl. Physiol.* 86, 1311-1318 (1999a).
- Rasmussen, H., Tønnessen, T.I., Mirtaheri, P., Kvarstein, G., Johnsen, H., Dirven, H., and Midtvedt, T.: Bacterial activity, measured by P<sub>CO<sub>2</sub></sub> in the caecum of mice and effects of the dietary composition. *Microb. Ecol. Health Dis.* 11 (Suppl. 2), 106 (1999b).
- Rasmussen, H., Midtvedt, T., Grant D., Johnsen, H., and Dirven, H.: Cecal and hepatic lesions in mice and rats after intravenous administration of gas-carrier contrast agents. *J. Ultrasound Med.* 20 (Suppl.), S13 (2001).
- Rasmussen, H., Mirtaheri, P., Dirven, H., Johnsen, H., Kvarstein, G., Tønnessen, T.I., and Midtvedt, T.: PCO<sub>2</sub> in the large intestine of mice, rats, guinea pigs, and dogs and effects of the dietary substrate. *J. Appl. Physiol.* 92, 219-224 (2002).
- Rasmussen, H., Dirven, H., Grant D., Johnsen, H., and Midtvedt, T.: Etiology of cecal and hepatic lesions in mice after administration of gas-carrier contrast agents used in ultrasound imaging. *Toxicol. Appl. Pharmacol.* 188, 176-184 (2003).
- Ridgway, S.H. and Howard, R.: Dolphin lung collapse and intramuscular circulation during free diving: Evidence from nitrogen washout. *Science* 206, 1182-1183 (1979).
- Rozenfeld, R.A., Dishart, M.K., Tønnessen, T.I., and Schlichtig, R.: Methods for detecting local intestinal ischemic anaerobic metabolic acidosis by P<sub>CO<sub>2</sub></sub>. *J. Appl. Physiol.* 81, 1834-1842 (1996).
- Saltzman, H.A. and Sieker, H.O.: Intestinal response to changing gaseous environments: Normobaric and hyperbaric observations. *Ann. NY Acad. Sci.* 150, 31-39 (1968).
- Schlieff, R., Alhassan, A., Wiggins, J., Schumann, W., and Niendorf, H.-P.: Safety of the galactose-based ultrasound contrast agent Levovist®. Conference Proceedings CMR, Woodstock, VT (1999).
- Sebastia, C., Quiroga, S., Espin, E., Boye, R., Alvarez-Castells, A., and Armengol, M.: Portomesenteric vein gas: Pathological mechanisms, CT findings, and prognosis. *Radiographics* 20, 1213-1224 (2000).
- Sivarajah, A., McDonald, M.C., and Thiernemann, C.: The production of hydrogen sulfide limits myocardial ischemia and reperfusion injury and contributes to the cardioprotective effects of preconditioning with endotoxin, but not ischemia in the rat. *Shock* 26, 154-161 (2006).
- Sly, W.S. and Hu, P.Y.: Human carbonic anhydrase and carbonic anhydrase deficiencies. *Annu. Rev. Biochem.* 64, 375-401 (1995).
- Staub, N.C.: Transport of Oxygen and Carbon Dioxide. In *Basic Respiratory Physiology*. (Staub, N.C., Ed.). Churchill Livingstone, New York, 149-168 (1991).
- Steggerda, F.R.: Gastrointestinal gas following food consumption. *Ann. NY Acad. Sci.*

- 150, 57-66 (1968).
- Svendsen, P. and Carter, A.M.: Influence of injectable anaesthetic combinations on blood gas tensions and acid-base status in laboratory rats. *Acta Pharmacol. Toxicol.* 57, 1-7 (1985).
- Tønnessen, T.I.: Biological basis for PCO<sub>2</sub> as a detector of ischemia. *Acta Anaesthesiol. Scand.* 41, 659-669 (1997).
- Tønnessen, T.I. and Kvarstein, G.: PCO<sub>2</sub> electrodes at the surface of the kidney detect ischemia. *Acta Anaesthesiol. Scand.* 40, 510-519 (1996).
- Van Liew, H.D.: Oxygen and carbon dioxide permeability of subcutaneous pockets. *J. Appl. Physiol.* 202, 53-58 (1962).
- Van Liew, H.D.: Coupling of diffusion and perfusion in gas exit from subcutaneous pockets in rats. *Am. J. Physiol.* 214, 1176-1185 (1968).
- Van Liew, H.D. and Burkard, M.E.: Behaviour of bubbles of slowly permeating gas used for ultrasonic imaging contrast. *Investigative Radiology* 30, 315-321 (1995).
- Van Liew, H.D., Conkin, J., and Burkard, M.E.: The oxygen window and decompression bubbles: Estimates and significance. *Aviat. Space Environ. Med.* 64, 859-865 (1993).
- Van Liew, H.D. and Raychaudhuri, S.: Stabilized bubbles in the body: Pressure-radius relationships and the limits to stabilization. *J. Appl. Physiol.* 82, 2045-2053 (1997).
- Zanardo, R.C., Brancalone, V., Distrutti, E., Fiorucci, S., Cirino, G., and Wallace, J.L.: Hydrogen sulfide is an endogenous modulator of leukocyte-mediated inflammation. *FASEB J.* 20, 2118-2120 (2006).